

Schottky barriers in carbon nanotube heterojunctions

Arkadi A. Odintsov^{1,2}

¹*Department of Applied Physics and DIMES, Delft University of Technology, 2628 CJ Delft, The Netherlands*

²*Nuclear Physics Institute, Moscow State University, Moscow 119899 GSP, Russia*

(August 10, 2018)

Electronic properties of heterojunctions between metallic and semiconducting single-wall carbon nanotubes are investigated. Ineffective screening of the long range Coulomb interaction in one-dimensional nanotube systems drastically modifies the charge transfer phenomena compared to conventional semiconductor heterostructures. The length of depletion region varies over a wide range (from the nanotube radius to the nanotube length) sensitively depending on the doping strength. The Schottky barrier gives rise to an asymmetry of the I-V characteristics of heterojunctions, in agreement with recent experimental results by Yao *et al.* and Fuhrer *et al.* Dynamic charge build-up near the junction results in a step-like growth of the current at reverse bias.

PACS numbers: 71.20.Tx, 73.30.+y, 73.23.-b

Single-wall carbon nanotubes (SWNTs) are giant linear fullerene molecules which can be studied individually by methods of nanophysics¹. Depending on the wrapping of a graphene sheet, SWNTs can either be one-dimensional (1D) metals or semiconductors with the energy gap in sub-electronvolt range^{2,3}. While metallic nanotubes can play a role of interconnects in future electronic circuits, their semiconducting counterparts can be used as basic elements of switching devices. An example is the field effect transistor on semiconducting SWNT operating at room temperature⁴.

Of particular interest are all-nanotube devices⁵. The simplest can be fabricated by contacting two SWNTs with different electronic properties. The SWNTs can be seamlessly joined together by introducing topological defects (pentagon-heptagon pairs) into the hexagonal graphene network⁶. The resulting on-tube junction generically has the shape of a kink. Electronic properties of such junctions have been investigated theoretically (see e.g. Refs.^{7,8}) within the model of non-interacting electrons.

Electron transport in nanotube heterojunctions has been studied in two recent experiments. Yao *et al.* treated junctions in SWNTs with kinks⁹ whereas Fuhrer *et al.* explored contacts of crossed nanotubes¹⁰. Both groups observed non-linear and asymmetric $I - V$ characteristics resembling that of rectifying diodes. On one hand, the rectifying behavior can be naturally interpreted in terms of Schottky barriers (SBs). On the other hand, formation of a SB might be surprising since one expects no charge transfer in junctions between two SWNTs made of the same material.

A possible reason for the charge transfer might be the doping of the nanotubes forming the heterojunction¹¹. The doping can be caused by introduction of dopant atoms into the nanotubes or by charge transfer from metallic electrodes. In the latter case the doping strength can also be controlled by the gate voltage. It is important to mention that screening of the Coulomb interaction is ineffective in one-dimensional nanotubes. For this reason the effect of the doping is long-ranged: the density of the transferred charge decays slowly with the distance from the electrodes and might be appreciable at the heterojunction¹².

The long-range Coulomb interaction should be properly taken into account when treating the charge transfer in the heterojunction itself. Unfortunately, this was not accomplished in Ref.¹¹, where the electric field was assumed to be fully screened in the region of a few atomic layers near the junction. In this Letter we study charge transfer phenomena in nanotube heterojunctions with true long-range Coulomb interaction. We concentrate on the metal-semiconductor SWNT junction and analyze its equilibrium and non-equilibrium properties (SB parameters, I-V characteristics) by solving the Poisson equation self-consistently.

As a model system we consider "straight" junction¹³ between metallic ($x < 0$) and semiconducting ($x > 0$) SWNTs (Fig. 1). We assume that the conducting p_z electrons in SWNTs are confined to the surface of a cylinder of radius R . The nanotubes are surrounded by a coaxial cylindrical gate electrode of radius $R_s \gg R$. The Fourier components of the 1D Coulomb interaction are given by

$$U(q) = \frac{2e^2}{\kappa} \left\{ I_0(qR)K_0(qR) - \frac{I_0^2(qR)K_0(qR_s)}{I_0(qR_s)} \right\}, \quad (1)$$

with the dielectric constant of the medium κ and the modified Bessel functions I_0 , K_0 . Equation (1) describes the long-range Coulomb interaction, $U(x) = 1/\kappa x$, for $R \ll x \ll R_s$. The interaction is screened at large distances $x \gg R_s$, so that $U(0) = e^2/C = (2e^2/\kappa) \ln(R_s/R)$, C being the capacitance of SWNT per unit length. The kernel (1) relates the electrostatic potential φ at the surface of SWNTs to 1D charge density $e\rho$ ($e > 0$),

$$e\varphi_q = U(q)\rho_q. \quad (2)$$

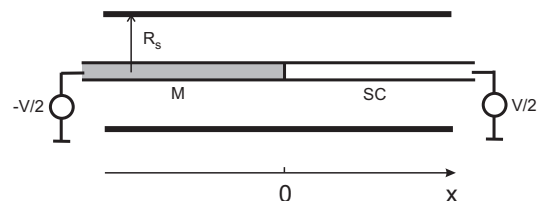


FIG. 1. Heterojunction between metallic (M) and semiconducting (SC) nanotubes. The potential V_g is applied to a cylindrical gate electrode of radius R_s

Since experimental values^{9,10} of the conductance of heterojunctions are small, $G/(e^2/h) \lesssim 10^{-2}$, we will assume low transparency $T \ll 1$ of the barrier between two SWNTs. In this case the electrons in the nanotubes are described by the equilibrium Fermi distribution $f(E)$, also when the voltage V is applied to the system.

In equilibrium, the charge density is related to the energy $\tilde{E}_0(x) = E_0(x) - E_F(x)$ of the gapless point (charge neutrality level) of graphite E_0 counted from the Fermi level E_F ,

$$\rho(x) = \int dE \text{sign}(E) \nu(E) f[(E - \tilde{E}_0(x)) \text{sign}(E)], \quad (3)$$

with the density of electronic states ν^{14} . Equation (3) is valid provided that $\tilde{E}_0(x)$ varies slowly on the scale of the Fermi wavelength.

We restrict our consideration to low energies $|\tilde{E}_0| < \Delta^{(1)}$, $k_B T \ll \Delta^{(1)}$ and neglect the effect of higher 1D subbands ($\Delta^{(1)}/(\hbar v_F/R) = 1, 2/3$ for metallic/semiconducting SWNT). The densities of states in metallic and semiconducting SWNTs are given by

$$\nu_M = \frac{4}{\pi \hbar v_F}, \quad \nu_S = \frac{4}{\pi \hbar v_F} \frac{|E| \Theta(|E| - \Delta)}{\sqrt{E^2 - \Delta^2}}, \quad (4)$$

with the Fermi velocity $v_F \simeq 8.1 \times 10^5$ m/s and the energy gap $2\Delta = 2\hbar v_F/3R$ in semiconducting SWNT ($\Delta \simeq 0.3$ eV for generic SWNTs² with $R = 0.5 - 0.7$ nm).

In the limit of zero temperature Eq. (3) may be inverted as,

$$\tilde{E}_0(\rho) = \begin{cases} \rho/\nu_M, & x < 0, \\ \sqrt{\Delta^2 + (\rho/\nu_M)^2}, & x > 0. \end{cases} \quad (5)$$

The charge neutrality level $\tilde{E}_0(x)$ is related to the electrostatic potential (2),

$$\tilde{E}_0(x) + e\varphi(x) = \mu + eV \text{sign}(x)/2, \quad (6)$$

$\mu \mp eV/2$ being the electro-chemical potentials for holes in metallic and semiconducting SWNTs. The potential $\mu = \alpha(\Delta W - eV_g)$ can be controlled by the gate voltage V_g (Fig. 1). It also incorporates the difference $\Delta W = W_M - W_{NT}$ of the work functions of the gate electrode and SWNT¹⁵ (the coefficient α characterizes mutual capacitance of the nanotubes to the gate and is equal to unity in our case).

We solve Eqs. (2), (3), (6) self-consistently by numerical minimization of the corresponding energy functional. The Coulomb energy is computed in the Fourier space. Figures 2, 3 display the results for the following parameters: $R_s/R = 75$ ($R_s \simeq 50$ nm for (10,10) SWNTs) and $\nu_M U(0)/\ln(R_s/R) = 5$. The latter value corresponds to the dielectric constant $\kappa \simeq 1.4$ which can be inferred from the experimental data (see Fig. 4 of Ref.¹).

The band bending diagrams (Fig. 2) display the charge neutrality level $\tilde{E}_0(x) = \tilde{E}_0(x) - eV \text{sign}(x)/2$ counted from the "average" Fermi level of metallic and semiconducting SWNTs, as well as the energies $E_{c,v} = \tilde{E}_0 \pm \Delta$

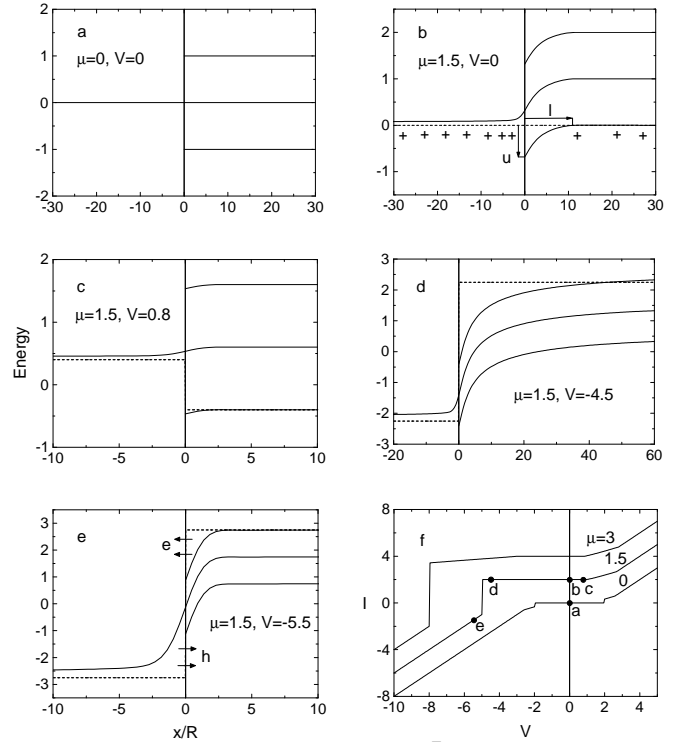


FIG. 2. The charge neutrality level \tilde{E}_0 and the energies of the conduction E_c and valence E_v bands as functions of the distance from the junction (a-e). The Fermi levels are shown by dashed lines. The $I - V$ characteristics of the heterojunction at zero temperature (f). The energies μ , eV are in units of Δ ; the current is in units of $2e\Delta T_i/(\pi\hbar)$. The $I - V$ curves for $\mu = 1.5, 3$ are offset for clarity.

of the conduction and valence bands in semiconducting SWNT. Let us start from the case of zero bias, $V = 0$ (Figs. 2(a), 2(b)). At zero electro-chemical potential, $\mu = 0$, the Fermi level of the nanotubes coincides with the gapless point of graphite and the system is charge neutral (Fig. 2(a)). This situation occurs for isolated nanotubes. The barriers for the electron and hole transport are equal to Δ (Fig. 3(a)).

To make contact with the experiments^{9,10} we will concentrate on p-doped SWNTs ($\mu > 0$). Due to larger number of electronic states $\int_0^{\tilde{E}_0} dE \nu(E)$ the metallic SWNT acquires more charge and has higher electrostatic potential $\varphi(-\infty)$ (lower charge neutrality level $\tilde{E}_0(-\infty)$) compared to semiconducting SWNT kept at the same electrochemical potential, see Eqs. (5), (6). The electric field induced by this charge bends the bands in the semiconducting part downwards so that a SB is formed near the interface (Fig. 2(b)).

For $|\mu| < \Delta$, there are no free charges in the semiconducting SWNT. Our numerical results indicate that the electrostatic potential $\varphi(x)$ decays logarithmically at $R \ll x \ll R_s$ so that the bend extends over long distances $x \sim R_s$ (the analytical estimate, $\varphi(x) \simeq e\nu_M \mu \ln(R_s/x)/\kappa$, is available in the limit of weak interaction, $\nu_M U(0) \ll 1$). At $\mu = \Delta$ holes enter the semiconducting SWNT. With increasing the electrochemical potential the holes come closer to the junction reducing the length l and the height u of a SB (Fig. 2(b)). In the case of weakly doped semiconducting

SWNT, $\mu = \Delta(1 + \delta)$, $\delta \ll 1$, a rough estimate of the depletion length l can be made, $\ln(l/R_s) \sim \delta \ln(R/R_s)$, for $R \ll l \ll R_s$. Therefore, the depletion length changes rapidly from $l \sim R_s$ to $l \sim R$ with increasing doping in this regime. The height of a SB can be estimated from the difference of the charge neutrality levels in semiconducting and metallic SWNTs, $u \lesssim \tilde{E}_0(\infty) - \tilde{E}_0(-\infty)$. The latter evaluate at $\tilde{E}_0(-\infty) = \mu/(1 + \nu_M U(0))$ and $\tilde{E}_0(\infty) = \Delta$ for $\delta \ll \nu_M U(0)$, see Eqs. (2), (5), (6). Since the band bending occurs predominantly in the semiconducting part (Figs. 2(a), 2(b)) and $\nu_M U(0) \gg 1$, one expects that $u \simeq \Delta$ for $\delta \ll \nu_M U(0)$. Note that SB persists up to remarkably large values of the electro-chemical potential, $\mu \approx 14\Delta$ (Fig. 3(a)) though it becomes rather short ($l < R$) for $\mu \gtrsim 8\Delta$.

Figure 3(a) shows the result for the SB height defined as the minimum energy of electron or hole excitation required to transfer the elementary charge across the junction in the absence of tunneling through the SB. The SB height shows pronounced asymmetry as a function of the bias voltage. Under a forward/backward bias the charge density in metallic SWNT decreases/increases. This reduces/enhances the band bending (Figs. 2(c), 2(d)) in the semiconducting part (the charge density and the band bending change sign for $V > 2\mu$, cf. Fig. 3(a)). As a result, the SB height decreases faster under a forward bias. This gives rise to the asymmetry $V_+ < |V_-|$ of positive V_+ and negative V_- threshold voltages at which SB vanishes ($u \rightarrow 0$) and the onset of the conductance occurs. The positive threshold voltage is relatively insensitive to the doping strength, Fig. 3(a). This can be used for a rough estimate of the gap Δ from experimental data, $\Delta \simeq eV_+$, for $\mu \sim 1$. Note that we assume weak interband tunneling in semiconducting SWNT so that the electronic states in the conduction band are empty in Fig. 2(d).

We will proceed with the analysis of non-equilibrium electron transport. The current through the heterojunction is given by the Landauer formula,

$$I = \frac{2e}{\pi\hbar} \int dE T(E) \{f(E - eV/2) - f(E + eV/2)\}, \quad (7)$$

with the energy-dependent transmission coefficient $T(E)$ of the junction. It is natural to separate the contribution $T_i(E)$ of a barrier at the interface between SWNTs⁸ and the contribution $T_S(E)$ of a SB to the total transmission. As a minimal model, we assume that the transparency T_i is energy independent whereas the transparency $T_S(E)$ increases from zero to unity when the energy E crosses the edge of a SB. In this case the total transmission reads $T(E) = 0, (T_i)$, for the energies in (out of) the SB range $[E_{\min}, E_{\max}]$. In the case of downward bending (Fig. 2) the SB range is given by $[E_v(0), E_c(\infty)]$, in the absence of charge carriers in the conduction band, $\mu + eV/2 > -\Delta$ (Figs. 2(a-d)), and by $[E_v(0), E_c(0)]$, in their presence, $\mu + eV/2 < -\Delta$ (Fig. 2(e)). The results for the $I - V$ characteristics at zero temperature are presented in Figs. 2(f), 3(b).

With increasing forward bias the SB (Fig. 2(c)) disappears and the hole transport channel opens at $V > V_+$.

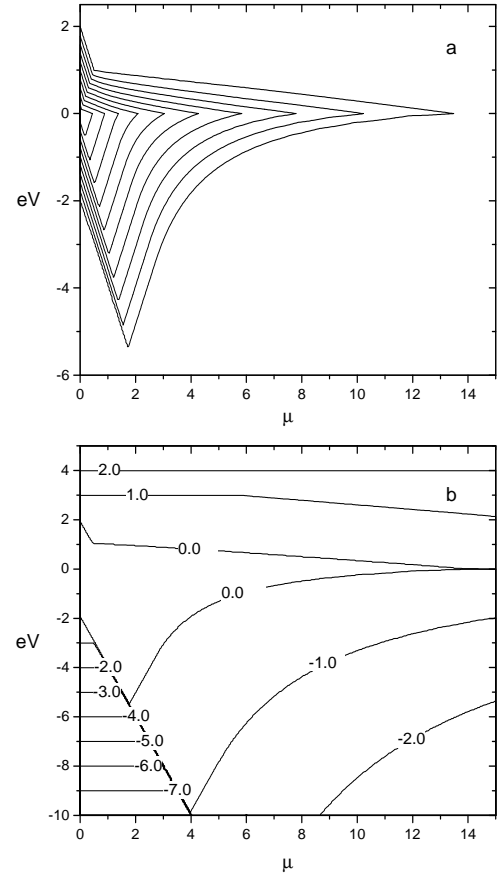


FIG. 3. The height u of the Schottky barrier (a) and the current through the heterojunction (b) at zero temperature. The contour lines (a) correspond to $u/\Delta = 0, 0.1, \dots, 0.9$ from periphery to origin. The energies μ , eV are in units of Δ . The current is in units of $2eDT_i/(\pi\hbar)$.

The cusp at the $I - V$ characteristics (Fig. 2(f)) at somewhat higher voltages corresponds to the onset of the electron channel. Note that at high (forward or reverse) bias both the electron and hole channels are open and the current is given by $I = (2eT_i/\pi\hbar)[eV - 2\Delta \text{sign}(V)]$.

The onset of the conductance under reverse bias depends critically on the electro-chemical potential μ (Figs. 2(f), 3(b)). At low doping, $\mu \lesssim 1.8\Delta$, the current increases abruptly at $V_- = V_c$, $eV_c = -2(\Delta + \mu)$. The voltage V_c corresponds to the alignment of the Fermi level with the conduction band of semiconducting SWNT. Electrons entering the conduction band cause the charge build-up near the junction. The reconstruction of the band profile (cf. Figs. 2(d) and 2(e)) results in the onset of the electron and hole channels of transport giving rise to a step-like growth of the current. At higher doping, $\mu \gtrsim 1.8\Delta$, the threshold voltage $V_- > V_c$ corresponds to the opening of the hole channel. The current gradually grows under reverse bias $V_c < V < V_-$ until the reconstruction of the band profile occurs at $V = V_c$ (see the curve for $\mu = 3$ in Fig. 2(f)).

We now consider quantum tunneling through the SB. The transparency $T_S(E)$ of the SB can be evaluated using WKB method and the effective mass approximation. For a triangular barrier of the length l and the height u we obtain,

$$T_S \sim \exp\left(-\frac{4l}{9R}\sqrt{\frac{2u}{\Delta}}\right). \quad (8)$$

The transparency T_S increases considerably near the boundaries of the transport blockade region $[V_-, V_+]$ (Fig. 3(a)) due to decreasing u and l . For example, $T_S \sim 2.5 \times 10^{-3}$ for the SB in Fig. 2(b), whereas $T_S \sim 1$ for the SBs in Figs. 2(c), 2(d). This gives rise to a substantial leakage current in the blockade region.

The asymmetry of the $I - V$ characteristics and threshold voltages has been discovered in recent experiments^{9,10}. According to the data of Ref.⁹, both the thresholds V_+ , V_- shift upwards with the gate voltage. Moreover, the positive threshold shifts less than the negative one. Such behavior is consistent with our model in the regime of moderate doping, $0.5 < \mu/\Delta \lesssim 1.8$ (Fig. 3). However, the blockade region of 3 – 4 V detected in the experiment is somewhat wider than the theoretical estimate, $V_+ - V_- \lesssim 6.5\Delta \simeq 2$ eV. The extra voltage drop could be due to potential disorder in semiconducting SWNT¹⁶ and/or an additional SB at the interface between semiconducting SWNT and metallic electrode.

We now check the model against the experimental data of Ref.¹⁰. The measured width of the blockade region, 0.5 – 0.7 V, agrees with the theoretical estimate. The gap in semiconducting SWNT, $\Delta \simeq eV_+$, evaluates at $\Delta = 0.19, 0.29$ eV for the two devices studied¹⁰. These values are in the expected range $\Delta \sim 0.25 - 0.35$ eV^{2,3}. A smooth onset of the current over the range $\sim 0.1 - 0.3$ eV around threshold voltages is naturally associated with quantum tunneling through a "leaky" SB (thermal energies are much smaller, $k_B T \simeq 5$ meV). Finally, the step-like feature of the current under reverse bias almost certainly corresponds to the reconstruction of the band profile due to the Fermi level entering the conduction band of semiconducting SWNT. Gradual onset of the differential conductance following the reconstruction might be associated with increasing conductance of disordered semiconducting SWNT under the doping¹⁶.

To conclude, we have studied the electronic properties of carbon nanotube heterojunctions and provided explanation for the main features of recent experimental data^{9,10}. Due to the long-range Coulomb interaction, the charge transfer phenomena in one-dimensional nanotube systems differ drastically from those in conventional semiconductor heterostructures. This creates new challenges in the design of novel electronic devices. In particular, the long-range electrostatic potential in underdoped junctions might affect other components of a circuit, whereas substantial leakage current in overdoped junctions spoils the rectification. In view of these challenges a new concept of functional devices on molecular level might be needed.

In the process of writing this paper I became aware of the preprint by Léonard and Tersoff¹⁷ who investigated equilibrium properties of junctions between semiconducting SWNTs and found the long-range charge-transfer phenomena in these systems (see also Ref.¹²).

The author wishes to thank B.L. Altshuler, G.E.W. Bauer, Yu.V. Nazarov, S. Tarucha, Y. Tokura, Z.Yao, and, especially, C. Dekker and P. McEuen for stimulating

discussions. F. Léonard and J. Tersoff are acknowledged for sharing the results of Ref.¹⁷ before publication. This work was supported by the Royal Dutch Academy of Sciences (KNAW).

-
- ¹ For a recent review see C. Dekker, *Physics Today* **5**, 22 (1999).
 - ² J.W.G. Wildöer, L.C. Venema, A.G. Rinzler, R.E. Smalley, and C. Dekker, *Nature* **391**, 59 (1998).
 - ³ T.W. Odom, J. Huang, P. Kim, and C.M. Lieber, *Nature* **391**, 62 (1998).
 - ⁴ S.J. Tans, A.R.M. Verschueren, and C. Dekker, *Nature* **393**, 49 (1998).
 - ⁵ M. Dresselhaus, *Physics World* **5**, 18 (1996).
 - ⁶ B.I. Dunlap, *Phys. Rev. B* **49**, 5643 (1994).
 - ⁷ Ph. Lambin, A. Fonseca, J.P. Vigneron, J.B. Nagy, and A.A. Lucas, *Chem. Phys. Lett.* **245**, 85 (1995).
 - ⁸ L. Chico, L.X. Benedict, S.G. Louie, and M.L. Cohen, *Phys. Rev. B* **54**, 2600 (1996).
 - ⁹ Z. Yao, H. Postma, L. Balents, and C. Dekker, to be published in *Nature*.
 - ¹⁰ M.S. Fuhrer, J. Nygård, L. Shih, M. Bockrath, A. Zettl, and P. McEuen, submitted to *Nature*.
 - ¹¹ A.A. Farajian, K. Esfarjani, and Y. Kawazoe, *Phys. Rev. Lett.* **82**, 5084 (1999).
 - ¹² A.A. Odintsov, Y. Tokura, to be published in *Proceedings of the LT-22, Helsinki, 1999*, preprint cond-mat/9906269.
 - ¹³ We expect the results to be qualitatively correct for heterojunctions with angles $\chi \gtrsim \pi/2$.
 - ¹⁴ In Eq. (3) ρ is averaged over few atomic distances. Our approach does not describe phenomena at atomic lengthscale, for instance, the Friedel oscillations.
 - ¹⁵ We assume that the charges at the nanotube and the gate electrode are not compensated by e.g. atmosphere ions, see L.D. Landau and E.M. Lifshitz, *Electrodynamics of Continuous Media*, Pergamon Press 1960, Ch. 3.
 - ¹⁶ P.L. McEuen, M. Bockrath, D.H. Cobden, Y. Yoon, and S.G. Louie, preprint cond-mat/9906055.
 - ¹⁷ F. Léonard and J. Tersoff, preprint.